

“FLYING” RF UNDULATOR *

I. V. Bandurkin, S. V. Kuzikov, A. V. Savilov[#], A. A. Vikharev,
Institute of Applied Physics, Nizhny Novgorod, Russian Federation

Abstract

A concept for the room-temperature rf undulator, designed to produce coherent X-ray radiation by means of a relatively low-energy electron beam and pulsed mm-wavelength radiation, is proposed. The “flying” undulator is a high-power short rf pulse co-propagating together with a relativistic electron bunch in a helically corrugated waveguide. The electrons wiggle in the rf field of the -1st spatial harmonic with the phase velocity directed in the opposite direction in respect to the bunch velocity, so that particles can irradiate high-frequency Compton’s photons. A high group velocity (close to the speed of light) ensures long cooperative motion of the particles and the co-propagating rf pulse.

INTRODUCTION

Typically, the undulator of an X-FEL is a periodic system of DC magnets with a magnetic field ~ 1 T and a period of several centimeters, where a wiggling relativistic electron bunch produces short wavelength radiation in the self-amplified spontaneous emission (SASE) regime [1-3]. In comparison with this traditional undulator, the so-called rf undulator, where an electron bunch flies toward a counter-propagating rf wave, introduces a strong appeal to use less energetic electron beam in order to produce the same wavelength of Compton’s scattered radiation [4-7]. In the case of weak electron wiggling, the wavelength of Compton’s photons produced by electrons with the same energy $W = mc^2(\gamma - 1)$, is determined by $\lambda \approx \lambda_{\text{rf}} / 4\gamma^2$ for the rf undulator (in contrast to $\lambda \approx \lambda_{\text{u}} / 2\gamma^2$ for the conventional undulator), where λ_{rf} and λ_{u} are the wavelength of microwaves for the rf undulator and the period of DC magnets for the conventional undulator, respectively. In order to reach the nanometer wavelength scale, one can use an electron bunch with an energy of several hundreds MeV in the rf undulator with a period of about ~ 1 cm instead of the 1-2 GeV beam in the conventional undulator with a period of several centimeters [8]. The effective undulator period can be as short as the wavelength of the used rf radiation, i.e., $\lambda_{\text{u}} = 2\pi / (h + k)$ (here, $k = \omega / c$ is the vacuum wavenumber, and h is the wave propagation constant). That is why millimeter and sub-millimeter radiation is preferable for the rf undulator.

The inevitable cost of these evident advantages is a necessity to provide a high power level of microwaves in order to ensure that an acceptable value of the undulator

parameter K is competitive with conventional undulators with $K \sim 1$. In the Ka-band, the necessary power of a wave (for it to be counter-propagating to electrons) in the waveguide with a radius of ~ 1 cm reaches a GW level. In order to provide such a power level, modern projects of rf undulators employ cavities with high Q-factors powered by existing high-power rf sources like klystrons or gyroklystrons, which are able to provide tens of megawatts. According to such a concept, the whole rf-undulator system should consist of many relatively short (~ 1 m) and mutually phased sections. As each section should be fed by its own rf source, the X-FEL consisting of tens of sections is very expensive.

Note that high-Q cavities bring a threat of destructive phenomena like rf breakdown and pulsed heating [9,10]. In order to avoid these undesirable phenomena, a short pulse of rf radiation of a high (GW) power level is preferable. In particular, experiments with particle accelerators show that nanosecond rf pulses of the GW level can travel through an electrodynamic structure without a breakdown [11].

There are necessary rf sources of the GW power level. In particular, these sources can be based on moderately-relativistic (hundreds of keV) BWOs [12-14]. Existing sources can deliver more than a 1 GW power in the X-band and about 1 GW in the Ka-band with a repetition rate as high as several kHz. It was proven experimentally that phases of these separate sources can be mutually locked [13]. The mentioned BWOs are able to produce rf radiation in short pulses only (usually shorter than 20 ns). If such a short rf pulse with the duration τ and the group velocity v_{gr} propagates counter to electrons in a waveguide, moving with a velocity close to the light velocity c then the effective undulator length for wiggling (the length of the intersection of electron path and rf pulse) is determined as follows

$$L_{\text{eff}}^{\text{count}} = \frac{v_{\text{gr}}\tau}{1 + v_{\text{gr}}/c}. \quad (1)$$

If $\tau = 10$ ns, $v_{\text{gr}} \approx c$, then $L_{\text{eff}} \approx 1.5$ m. This is too short for the SASE XFEL, so that a lot of sections and rf sources are required to reach the saturation level.

CONCEPT OF THE FLYING UNDULATOR

We suggest an rf undulator based on co-propagation of an electron bunch and a short high-power rf pulse without a loss in Doppler’s up-conversion of the frequency [15]. This “flying” undulator has the following effective undulator length:

*Work supported by the Russian Foundation for Basic Research (Projects 14-08-00803 and 14-02-00691).

[#]savilov@appl.sci-nnov.ru

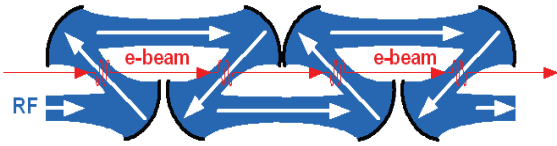


Figure 1: Periodic mirror transfer line with the “flying” rf undulator.

$$L_{\text{eff}}^{\text{co}} = \frac{v_{\text{gr}}\tau}{1 - v_{\text{gr}}/c}, \quad (2)$$

which is longer by factor $(1 + v_{\text{gr}}/c)/(1 - v_{\text{gr}}/c)$ than the interaction distance of the counter-propagating particles and the rf pulse with the same duration. The sectioned scheme shown in Fig. 1 illustrates the main idea of the “flying” undulator. Electrons and the rf pulse (which naturally contains counter-propagating wave subsections) can move together over a long distance. However, the length of the counter-propagating subsections is small as compared to the length of the whole undulator.

CORRUGATED WAVEGUIDE MODES

In a helical corrugated waveguide (Fig. 2), wiggling can be provided in the long section. The surface of this waveguide can be described in the cylindrical system of coordinates (z -axis coincides with waveguide center) by the formula $r(z, \varphi) = R_0 + a \sin(2\pi z/D + \bar{m}\varphi)$, where R_0 is the average waveguide radius, a is the corrugation amplitude, D is the period, and \bar{m} is the number of helical threads. In this corrugated waveguide, there is an infinite number of the so-called Floquet’s spatial harmonics with propagation constants $h_n = h_0 + 2\pi n/D$ (here n is the harmonic number) and phase velocities $v_{\text{ph}} = \omega/h_n$ (they could be either positive or negative relative to the electron velocity sign).

We consider the “flying” rf undulator, where the co-propagating 0-th harmonic has the positive propagation constant h_0 and phase velocity, but the -1-st harmonic has the negative propagation constant h_{-1} and the negative phase velocity. The group velocity is positive and constant for all spatial harmonics. Particles are assumed to oscillate in the transverse fields of the -1-st harmonic. In this case, the equivalent undulator period is given by the formula

$$\lambda_u = 2\pi / (|h_{-1}| + k). \quad (3)$$

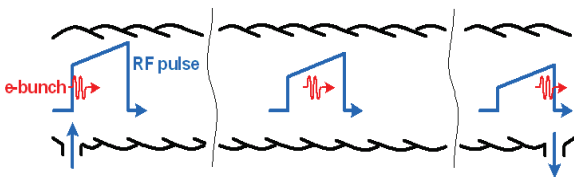


Figure 2: “Flying” rf undulator based on the helical waveguide.

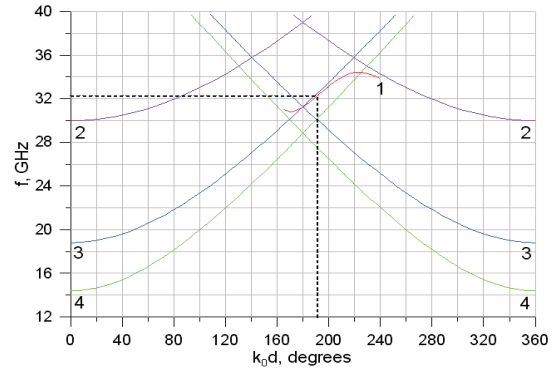


Figure 3: Dispersion characteristic of the normal TM_{01} - TM_{11} wave in the helical waveguide (curve 1); dispersion curves of TM_{11} (2), TM_{01} (3), and TE_{11} (4) partial waves in the smooth circular cross-section waveguide.

Note that $|h_{-1}|$ can be close to the vacuum wavenumber k , or even bigger (for slow -1st harmonic). Therefore, the equivalent undulator period might be favourably as short as it is in the case of the counter-propagating rf pulse (when the equivalent undulator period is close to the half-wavelength, $\lambda_u = 2\pi/(h+k) \approx \lambda_{\text{rf}}/2$).

Eigenmodes of a helical waveguide with a weak corrugation can be represented using partial waves of the smooth circular waveguide. Far from Bragg’s resonances, amplitudes of all non-zero harmonics are negligibly small. Nevertheless, if Bragg’s conditions ($h_1 \pm 2\pi/D = h_2$ and $m_1 \pm \bar{m} = m_2$, where h_1, h_2 are propagation constants of partial modes, and m_1 and m_2 are azimuthal indices) is satisfied for a certain pair of waves, the amplitudes of 0-th and ± 1 -st harmonics become comparable.

The co-propagating partial wave of the “flying” undulator can cause large-scale perturbation of electron motion and spoil the X-FEL radiation spectrum [8]. In order to avoid this, the 0-th and -1-st harmonics should be represented by modes with different transverse structures. The 0-th harmonic should be chosen so that it does not have transverse fields in the center, where a thin electron beam is injected. Waves like $\text{TE}_{m,n}$ or $\text{TM}_{m,n}$ with the azimuth index $m \neq 1$ satisfy this requirement. Of course, the operating (“wiggling”) fields of the -1-st harmonic should be as high as possible. Therefore, the -1-st harmonic should preferably be a wave with $m=1$. In particular, let us consider the rf undulator based on the helical corrugated waveguide, where the TM_{01} wave is actually the 0th harmonic, the rotating TM_{11} is the -1-st harmonic in the one-thread ($\bar{m} = 1$) helical waveguide.

We investigate the operating TM_{01} - TM_{11} wave. Figure 3 illustrates the dispersion curve of this normal wave (the eigenfrequency vs the phase $h_0 D$ in degrees) for the following waveguide parameters: $R_0=6.1$ mm, $D=6$ mm, and $a=0.3$ mm. Dispersion curves of the main partial modes in the smooth circular waveguide are also shown.

The dispersion curve of our normal wave is close to linear within the phase interval between 170° and 220° . At these points, the dispersion curve of the partial TM_{01} mode has intersections with the dispersion curves of the partial TM_{11} and TE_{11} waves, correspondingly. Thus, at these points one can observe the phenomenon of the dispersion curve's splitting caused by Bragg's resonance. Note that the operating point is placed approximately between the mentioned TM_{01} - TM_{11} and TM_{01} - TE_{11} Bragg's resonances, so that the TE_{11} fields contribute also to the field structure of the operating normal wave.

FLYING UNDULATOR OPTIMIZATION

The dimensionless magnitude of the momentum of electron oscillations (the undulator parameter, $K = \gamma \mathcal{V}_\perp / c$) is proportional to the deflecting rf fields of the -1-st harmonic:

$$K = \frac{e(E_\perp + H_\perp)\lambda_u}{2\pi mc^2},$$

where E_\perp and H_\perp are the transverse fields at the waveguide axis. In a FEL, the amplitude of the optical radiation grows along the electron path on the z coordinate as $P_s = \exp(z/L_g)$, where the small-signal gain length, $L_g = (\sqrt{3}C/2)^{-1}$, is determined by the amplification parameter [16]

$$C = \left[K_{\text{eff}}^2 \frac{I}{I_A} \frac{4\pi}{\gamma^5 \sigma \lambda} \right]^{1/3}. \quad (4)$$

Here, I is the electron current, $I_A = 17 \text{ kA}$, and σ is the transverse rms size of the electron beam. In this formula, $K_{\text{eff}} = K$ in the case of a planar undulator. It is important that in the "flying" undulator, the wiggling component of the rf field has circular polarization; this makes the effective undulator parameter twice as high, $K_{\text{eff}} = 2K$.

Thus, the optical wave gain is $\exp(L_{\text{eff}}/L_g)$. At fixed parameters of the electron beam and rf pulse duration, L_{eff}/L_g is proportional to the factor

$$\eta = K^{2/3} \frac{v_{\text{gr}}/c}{1 - v_{\text{gr}}/c}, \quad (5)$$

which should be used to optimize parameters of the co-propagating "flying" rf undulator, as well as to compare the "flying" undulator with the rf undulator based on the counter-propagating wave [in the latter, factor η can be calculated by substituting the denominator in (5), namely, $\eta = K^{2/3} (v_{\text{gr}}/c)/(1 + v_{\text{gr}}/c)$].

Figure 4 shows the undulator parameter K , the normalized group velocity v_{gr}/c , and the gain parameter η calculated in accordance with Eq. 5 for the 1 GW rf power. The highest value of η (near 190° at $f=32 \text{ GHz}$) corresponds to $\lambda_u = 5.4 \text{ mm}$ and $v_{\text{gr}}/c \approx 0.7$. The maximum of η corresponds approximately to the maximum of v_{gr} , although K naturally grows up when the phase approaches to the Bragg's resonances mentioned above. The reason is that in accordance with Eq. 5 the vicinity of the group velocity to the light velocity is more vulnerable in comparison with the contribution of the rf field amplitude to the power of $2/3$. At the optimal point (190°) the ratio of the transverse electric field (32 MV/m) to the longitudinal one (102 MV/m) at the axis is 0.31. This value allows evaluating amplitudes of the partial TM_{11} wave ($E_z = 0, E_\perp \neq 0$) and the TM_{01} wave ($E_z \neq 0, E_\perp = 0$) in the normal wave.

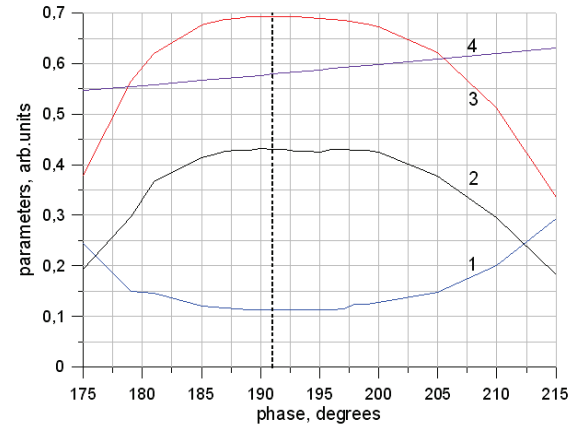


Figure 4: Normalized characteristics of the TM_{01} - TM_{11} normal wave in the helical waveguide undulator parameter K (curve 1), gain factor η (2), normalized group velocity v_{gr}/c (3), and the ratio of the effective undulator period to the rf wave wavelength radiation $\lambda_u/\lambda_{\text{rf}}$ (4).

Let us compare this "flying" rf undulator created on the basis of a 10 ns rf pulse with $\lambda_{\text{rf}} = 1 \text{ cm}$ and with the DC-magnet undulator ($K = 0.5$ and $\lambda_u = 3 \text{ cm}$). Due to $v_{\text{gr}} = 0.7c$, the "flying" undulator provides electron wiggling within the distance $L_{\text{eff}} \approx 10 \text{ m}$ (see Eq. 2) with the effective undulator period $\lambda_u = 0.58\lambda_{\text{rf}}$. At a fixed target radiation wavelength $\lambda \approx \lambda_u/2\gamma^2$, the ratio of the required electron energies is $\gamma^{\text{DC}}/\gamma^{\text{rf}} = \sqrt{\lambda_u^{\text{DC}}/\lambda_u^{\text{rf}}} = 2.3-2.5$. Since the amplification factor is proportional to $C \propto (K_{\text{eff}}^2/\gamma^5)^{1/3}$ and $K_{\text{eff}} = 2K$ for the circular polarized rf undulator,

one obtains $C^{rf}/C^{DC} = 2.3-2.6$. Thus, the “flying” rf undulator with $L_{eff} \approx 10$ m provides the gain, which is equally as high as the referenced DC undulator with the length $L \approx 25$ m, and requires significantly lower electron energy.

FOCUSSING PROPERTIES

We should mention an additional advantage of the “flying” undulator, namely, its focusing properties. The transverse fields of its co-propagating partial wave TM_{01} (0-th spatial harmonic) component have minimum (zero) at the waveguide axis (the e-beam position). Therefore, the pondermotive Miller force caused by this non-synchronous wave is directed to the centre (Fig. 5).

In contrast, the field of the operating undulator partial wave TM_{11} (-1-st spatial harmonics) possesses de-focusing properties (Fig. 5), as it has maximum in the centre of the operating waveguide. However, the estimated value of the de-focusing Miller force caused by this wave is significantly smaller as compared to the focusing force provided by the 0-th TM_{01} spatial harmonic.

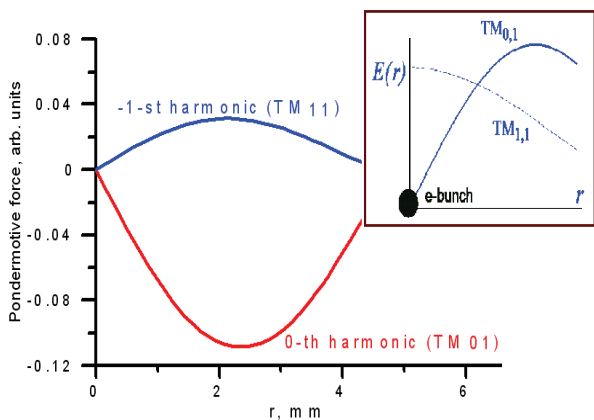


Figure 5: Transverse structures of the partial waves TM_{01} and TM_{11} forming the normal wave in the helical waveguide, and transverse structures of pondermotive Miller forces provided by these two partial waves.

RF SOURCE FOR THE FLYING UNDULATOR

As a prototype of the rf source for the flying undulator, a relativistic Cherenkov backward-wave oscillator is being under creation at the Institute of Applied Physics (Fig. 6). This rf source is based of the 550 kV / 4 kA electron beam provided by the SINUS-6 accelerator. A tubular beam of rectilinearly moving particles passes through the operating corrugated waveguide in a guiding magnetic field of 6 T and excites the backward far-from-cutoff operating mode TM_{01} . A special resonant reflector is placed at the waveguide input; this is needed to provide output of the rf power.

According to simulations, realization of the simplest scheme of such rf oscillator at the operating frequency of 35 GHz can be a way for creation of a source of a 20 ns rf

pulse with the peak power of about 0.5 GW; the corresponding electronic efficiency amounts $\sim 20\%$. According to simulations, the use of a sectioned operating cavity can enhance the output power up to 700-800 MW.

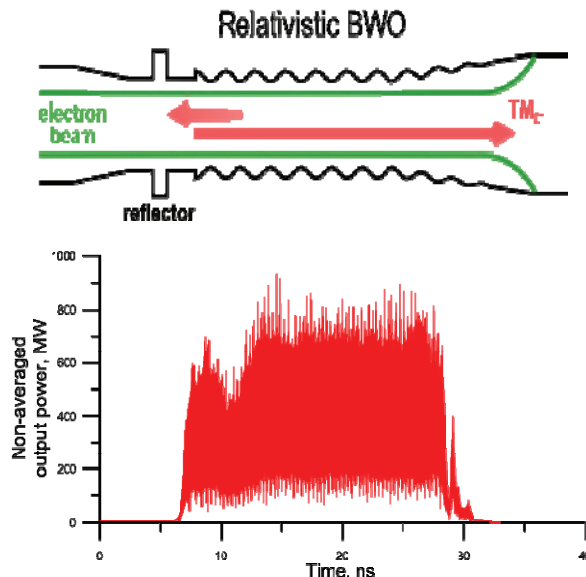


Figure 6: Relativistic Cherenkov BWO, and calculated non-averaged output power versus the time.

REFERENCES

- [1] L. Giannessi et al, Phys. Rev. Lett. 106, 144801 (2011).
- [2] C Bostedt et al., J. of Phys. B 46 , 164003 (2013).
- [3] G. Marcus et al., Appl. Phys. Lett. 101 , 134102 (2012).
- [4] V.L. Bratman, N.S. Ginzburg, M.I. Petelin, JETP Letters 28, 190 (1978).
- [5] T. Shintake et al, Japanese J. of Appl. Phys. 22, 844 (1983).
- [6] P. Sprangle, B. Hafizi and F. Mako, Appl. Phys. Lett. 55, 2559 (1989).
- [7] S. Tantawi et al, Phys. Rev. Lett. 112, 164802 (2014).
- [8] S. V. Kuzikov et al, Phys. Rev. ST Accel. Beams 16, 070701 (2013).
- [9] V. Dolgashev, S. Tantawi, Y. Higashi, and B. Spataro, Appl. Phys. Lett. 97, 171501 (2010).
- [10] L. Laurent et al, Phys. Rev. ST Accel. Beams 14, 041001 (2011).
- [11] M. C. Thompson et al, Phys. Rev. Lett. 100, 214801 (2008).
- [12] S. D. Korovin et al, Phys. Rev. E 74, 016501 (2006).
- [13] V.V. Rostov et al, Appl. Phys. Lett. 100, 224102 (2012).
- [14] A.V. Savilov, Appl. Phys. Lett. 97, 093501 (2010).
- [15] S.V. Kuzikov, A.V. Savilov, A.A. Vikharev, Appl. Phys. Lett. 105, 033504 (2014).
- [16] Zh. Huang and K.-J. Kim, Phys. Rev. ST AB 10, 034801 (2007).